

NUMERICAL OPTIMIZATION OF HELICOPTER ROTOR AERODYNAMIC PERFORMANCE IN HOVER

A. Le Pape, P. Beaumier

ONERA, Applied Aerodynamic Department
Châtillon, France

Abstract

An optimization procedure for helicopter rotor aerodynamic performance is presented. This optimization procedure is centered on the numerical optimizer CONMIN, a gradient-based method, that minimizes a functional under constraints. The optimizer has been coupled to a 3D Navier-Stokes CFD solver *elsA*, and applied to helicopter rotor optimization in hover.

The optimization chain and its components are first described. Several validations and applications are then presented starting from the 7A and 7AD rotor geometries with optimization of the different blade shape parameters (twist, chord, sweep and anhedral distribution). The efficiency and the robustness of the method are then tested for some more complex applications starting from the ERATO rotor. Finally a synthesis is made showing that the optimization chain is an helpful tool for the design of new helicopter rotors.

Notations

b	number of blades
c	local chord
c^*	reference chord
$Cb = \frac{100.C}{\frac{1}{2}\rho_\infty S \sigma R (R\Omega)^2}$	rotor torque coefficient
$CzM2$	2D sectional lift coefficient
$CxM3$	2D sectional power coefficient

$FM = \frac{T^{3/2}}{P\sqrt{2\rho_\infty S}}$	Figure of Merit
$FM = \frac{Zb^{3/2}}{20Cb}\sqrt{\sigma}$	
ρ_∞	density at infinity
R	rotor radius
r/R	spanwise location
$S = \pi R^2$	rotor disk surface
$\sigma = \frac{b.c^*}{\pi R}$	rotor solidity
T	rotor thrust
τ	linear aerodynamic twist
θ_c	collective pitch
x/c	chordwise location

$$Zb = \frac{100.Fz}{\frac{1}{2}\rho_\infty S \sigma (R\Omega)^2} \quad \text{rotor thrust coefficient}$$

Introduction

The design of helicopter rotor blades is a very complex task involving many domains and disciplines such as aerodynamics, acoustics, dynamics, which is not presently achieved in a single shot. Some attempts have been done in the recent past years to build optimization tools by coupling an optimizer algorithm with a

performance analysis code. Up to now, the aerodynamic performance are taken into account through models based on 1D momentum theory or lifting-line methods (Ref 1, 2, 3, 4). In parallel, the CFD methods have reached sufficient maturity to compute very accurately helicopter rotor aerodynamic performance in hover. These CFD methods are now currently applied during the design cycles of advanced geometry blades. The current CFD codes efficiency (CPU consumption, robustness, ...) enables to use them in automatic optimization chains. Such optimization strategies involving Navier-Stokes solvers have been applied in aeronautics on fixed wing configurations (Ref 5, 6), and via adjoint formulation on aircraft configurations (Ref 7, 8) and have demonstrated their efficiency to be successfully integrated in design cycles. Only few authors apply numerical optimization coupled with CFD codes on rotary wing, these automatic design tools being only applied for turbomachinery problems in quasi 3D and 3D (Ref 9, 10).

This paper describes an optimization strategy for helicopter rotor blades shape, based on the coupling of an optimizer (gradient method) with a 3D Navier-Stokes solver. For that purpose the CONMIN optimizer (Ref 11) has been coupled to the CFD object-oriented *elsA* software (Ref 12), developed by ONERA. The optimization procedure is focused on hover flight condition, since it is one of the critical point for the power and thrust required. In addition, for hover flight condition, only steady computations are required; at the present time, unsteady computations would not enable such a coupling because of a very high CPU time consuming. For comparison purpose and in order to assess the necessity to use CFD methods in such an optimization tool, applications are also made with CONMIN coupled with a lifting line code, HOST (Ref 13).

The description of the different functionalities of the optimization procedure is presented. First the general strategy for conducting the optimization, and the choice made are also explained. The validation of the coupling is performed on the optimization of linear aerodynamic twist of the 7A rotor, since the solution of this simple problem is well-known. Further applications on the optimization of the chord, sweep and anhedral distributions are then presented, and an analysis of the new geometries given by the optimizer is proposed. Finally the optimization chain is initialized by a more modern rotor shape: ERATO, for which the optimization of the blade tip is shown. A more complex optimization of the ERATO rotor involving several parameters and design variables concludes the study.

Optimization procedure

As shown on Figure 1, the optimization chain is composed of several elements centered on the coupling of the optimizer CONMIN with the CFD solver *elsA* and the lifting-line solver HOST.

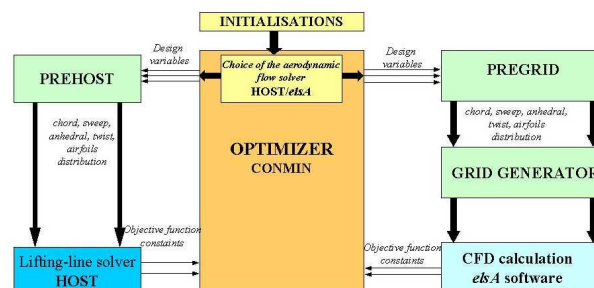


Figure 1: Flowchart of the optimization chain

The optimization procedure is based on the maximization of the Figure of Merit (FM) which quantifies the aerodynamic performance of a rotor in hover. This is achieved by the modification of different shape parameters such as twist (linear or not), chord, sweep, anhedral distributions or airfoils position along the blade span. The optimizer provides values of the design variables to the preprocessing routines that generate the new blade geometry. The aerodynamic performance of the new rotor is then evaluated by the flow solver to determine the objective function (Figure of Merit) and the constraints if necessary. The process is continued until an optimal design is reached.

CONMIN Optimizer

The optimization methods can be divided in two main types: the deterministic methods that reach the nearest local optimum, and the non-deterministic methods that are conceived to reach the global optimum. The main drawbacks of global methods is the number of objective function evaluations and the CPU time required. For example, the application of a gradient-based method in one hand, and a genetic algorithm in the other hand, on the optimization of a 2.5D section of compressor blade of an aircraft engine, shows that the genetic algorithm requires around 10 times more CFD computations. Because of this too high CPU time required, a local gradient-based method is chosen (Ref 10).

The optimizer used here is the CONMIN code, mainly used in such optimization strategy for aerodynamic topics. This is an efficient gradient-based method, where gradients are solved by finite differences at each optimization iteration. Three descent steps are performed per iteration to search for the objective function minimum with respect to the constraints by a feasible direction method

(projection of the design vector). By this way, for N_{it} CONMIN iterations, the flow solver is called $N_{it} \cdot (N_v + 3)$ times, where N_v is the number of design variables.

Design variables

The optimization chain is designed to optimize the following parameters defining helicopter rotor blades shape: chord, sweep, anhedral, twist distributions, and airfoils positions. Each of these parameters distribution can be optimized separately or combined one with another. The modifications can be applied all along the blade span or only on a specific part of the blade defined by the user.

Two types of parameterization of the blade shape can be used. The first possibility is to define the different parameter distributions with piecewise linear functions. This is the simpler way to define the blade geometry and in this case the design variables are the values of the chosen optimized distributions at the optimized spanwise locations.

The second possibility is to use interpolation functions. In the present optimization procedure, Bézier curves (Ref 14) have been used to define the blade shape geometry. These curves are well adapted to the shape design in aeronautics and are mainly used in aerodynamics optimization procedures (Ref 10). In this case, the design variables are the control points of the Bézier curves. This allows more complex shapes and smoother blade planforms with less design variables.

For all the optimizations performed, the rotor collective pitch θ_c is added as a design variable. By this way the rotor thrust is not fixed during the optimization process, and because the optimizer tries to reach the point of maximum of Figure of Merit, the final optimization point corresponds to the thrust for which the rotor efficiency (Figure of Merit) is maximum.

Grid Generation

When the *elsA* Navier-Stokes solver is used in the optimization, a grid has to be built at each new geometry evaluation. An analytical grid generator is used for that purpose. All the grids have a C-H monoblock topology with 121 points in the chordwise direction, 49 points in the spanwise direction (with 28 sections on the blade) and 33 points in the direction orthogonal to the blade surface, which makes a total of 195 657 points. Periodicity conditions allow to limit the computational domain to an azimuthal sector around one single blade, as shown on Figure 2 for the 7A rotor. The grid extension in the vertical direction is equal to $\pm 1.4R$ and to $2R$ in the spanwise direction. The size of the first cells on the

blade surface is chosen to have y^+ values around 3-4.

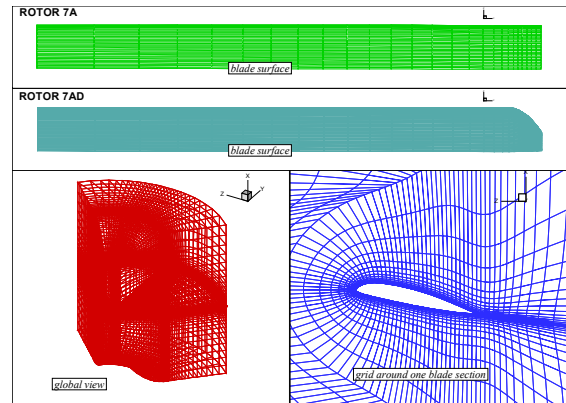


Figure 2: View of the optimization grid used for 7A and 7AD rotors

These computational grids are quite coarse in order to achieve reasonable CPU times for the full optimization process. In most of the cases, to assess the final result provided by the optimizer, the overall performance of the final rotor is computed on finer grids of 956 297 points (257x61x61). For these fine grids the size of the first cells on the blade surface is chosen to have y^+ values around 0.5-1.

Flow solvers

elsA

The *elsA* software, developed by ONERA, solves the Reynolds Averaged Navier-Stokes equations, written in a rotating cartesian coordinate system (for the present application) in a cell-centered finite volume formulation. A classical Jameson with 2nd order scheme discretization in space is used, with the addition of an artificial viscosity. The time integration is ensured by an implicit LU algorithm used with a backward Euler scheme. The convergence is improved by a 3-levels W-cycles multigrid method. Specific boundary conditions are imposed on the inflow/outflow boundaries, based on the 1D Froude theory. This is done so to ensure the evacuation of the rotor downwash and avoid non-physical recirculations in the computational domain. The turbulence is modeled with an algebraic model of Michel and the transition is prescribed at $x/c=0.15$ on the suction side and around $x/c=0.80$ on the pressure side (Ref 15). The prescription of the transition and the use of a simple turbulence model allow to perform several successive computations with a relatively low CPU consuming as required by the optimization procedure. In addition, each computation in the optimization process is initialized by the converged previous computation. As two consecutive geometries proposed by the optimizer are often

very close (for example during the gradients calculations), this strategy of initialization ensures a good robustness and convergence for each CFD computation.

For the computations on fine grids, a more accurate turbulence model is chosen. A $k-\omega$ (Wilcox) model with a SST correction is used. As shown on Figure 3, the computations of the 7A rotor using both coarse and fine grids (with the two turbulence model) are in a good agreement with experiment. The assumption to compute the flowfield on a coarse mesh during the optimization process is so reinforced. Nevertheless, the optimized rotor performance will be checked on fine grids, in most of the cases. Actually, the $k-\omega$ SST turbulence model enables to detect more accurately the stall at high thrust coefficients.

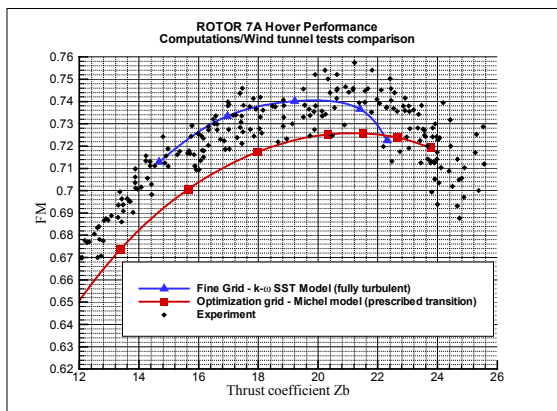


Figure 3: FM/Zb curves computed on 7A rotor and experiment

HOST

The HOST code (Helicopter Overall Simulation Tool) (Ref 13) was developed by Eurocopter France in order to simulate and analyze the behavior of an isolated rotor or a complete helicopter in various flight conditions. HOST may be used as a dynamic code or as in the present study as an aerodynamic code. The aerodynamic model used is based on the lifting-line theory. Given the trim (collective pitch) by the optimizer, the sectional Mach numbers and angles of attack are calculated, in order to determine aerodynamic coefficients from 2D airfoils tables. In hover, the induced velocity is then computed using a 1D momentum theory with a vortex ring model.

Rigid/soft blade assumption

One another functionality that offers the HOST code, is the calculation of the dynamic property of the rotor. At each optimization step, given the geometry and the collective pitch, the HOST code is able to compute the blade deformations (flap bending and torsion) and the rotor angles (flap and lead-lag). A new grid is then built around the

deformed blade and the CFD computation is performed. This coupling between the optimizer CONMIN and both the *elsA* software and the HOST code allow to perform optimization with the assumption of a soft blade, and so, to evaluate the influence on the optimization process of the rigid/soft blade assumption in hover.

Post-processing

After checking convergence of the flow solution, the *elsA* Navier-Stokes computation results are extracted by numerical integration of the pressure and viscous forces, as thrust coefficient (Z_b) and power coefficient (C_b) to compute the Figure of Merit, the objective function of the optimization process.

7A/7AD rotor Applications

First, the optimization chain is applied on the ONERA four-bladed 7A and 7AD rotors (Figure 2). These rotors have a radius of 2.1m and a chord of 0.14m, and the tip Mach number is 0.617. Beginning the optimization studies with these rotors is first chosen because of their very simple rectangular planform, with in addition a parabolic swept tip for the 7AD rotor.

Linear aerodynamic twist optimization

The first application is performed on the linear aerodynamic twist (1 design variable) of the 7AD rotor. This simple test-case is first addressed because the number of design variables is reduced to the minimum: the collective pitch (as in all the optimization runs) and the linear aerodynamic twist τ . In addition the solution of this problem is well-known since higher the aerodynamic twist is, better is the aerodynamic rotor performance in hover. In fact, increasing the linear twist reduces the lift in the outer part ($r/R > 0.7$) of the blade and increases the lift in the inner part. Consequently, the induced power is decreased (more uniform induced velocities distribution) and the intensity of the shock wave is reduced. This results in an important reduction of the power consumption of the rotor tip, and in an improvement of the aerodynamic efficiency.

Starting from the reference, $\tau = -8.3^\circ/R$ for the 7AD rotor, the upper and lower bounds for the linear aerodynamic twist are $\tau_{\min} = -18^\circ/R$ and $\tau_{\max} = 2^\circ/R$. As expected, the optimization procedure leads to the lower bound, the optimum value of $\tau_{\text{opt}} = -18^\circ/R$ as shown on Figure 4. The final rotor has its maximum of Figure of Merit improved by 4.6 points with the new optimized linear aerodynamic twist.

This proves the ability of the optimization procedure to reach the optimum solution of a

simple aerodynamic problem on the helicopter rotor in hover.

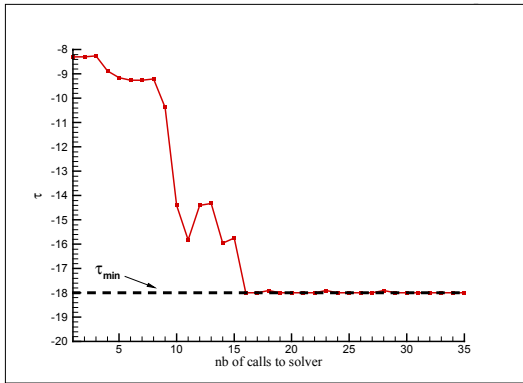


Figure 4: History convergence of the linear aerodynamic twist optimization

Chord distribution optimization

The optimization of the blade tip chord of the 7A rotor is performed by using 1 design variable at $r/R=1$. Bézier curves are chosen for the blade shape definition and realistic bounds are imposed for the chord value at $r/R=1$ (chord at blade tip should be between $0.3c^*$ and $2c^*$). This optimization of the chord distribution is done while keeping the rotor solidity constant. To achieve this, at each new geometry, the new chord distribution is adjusted in the preprocessing of the grid generation. If not, the optimization process may lead to a rotor with better performance only due to a solidity effect and not because a more suitable chord distribution.

The result of this optimization is presented on Figure 5. After the first optimization iteration, the optimizer reaches the lower bound of the blade tip chord. This reduction of the chord at the blade tip generates a slight increase of the chord in the main part of the blade (+1.5%) as the rotor solidity is fixed constant.

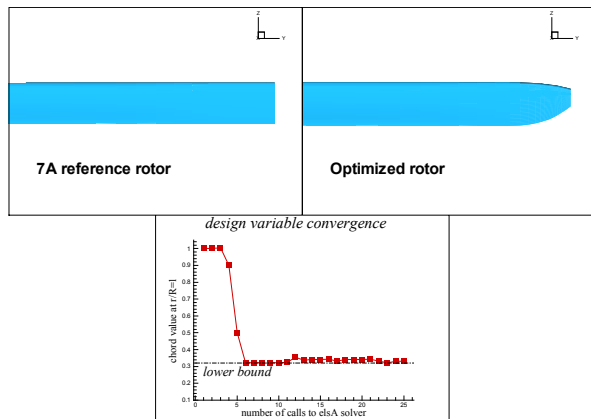


Figure 5: Optimization of 7A rotor blade tip chord

The performance of the optimized rotor is plotted on Figure 6, showing an improvement of 1.2 points of the maximum of Figure of Merit. Not only the performance at final thrust is enhanced, but the Figure of Merit is improved by approximately 1 point for all thrust coefficients. This improvement is mainly due to the redistribution of loads along the blade spanwise. The diminution of the blade tip chord leads to a diminution of lift in the outer part of the blade, and so, the intensity of the tip vortex is reduced. This redistribution of the airloads along the blade spanwise is illustrated on Figure 7, where are plotted the C_{zM2} and C_{xM3} for a thrust coefficient $Z_b=20$, near the maximum Figure of Merit.

This is also a known solution, and most of the recent rotor blades have a reduced tip chord as found by the optimization procedure.

This optimization has also been performed with the assumption of a soft blade by computing the blade deformation at each new geometry with the HOST code. The optimization process leads exactly to the same final geometry, showing that the rigid/soft blade assumption has, in this case, no influence on the optimization result.

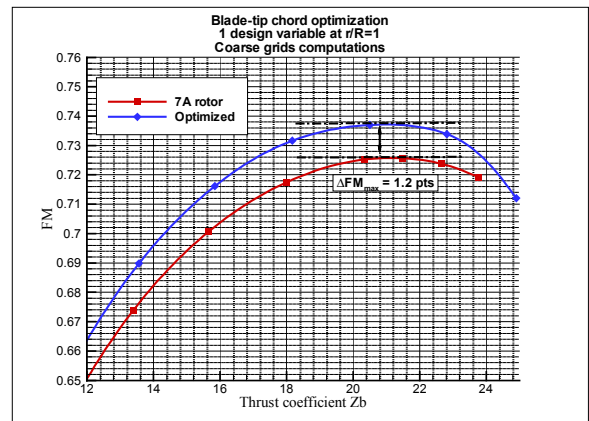


Figure 6: FM/Zb curve of the 7A rotor with optimized blade tip chord

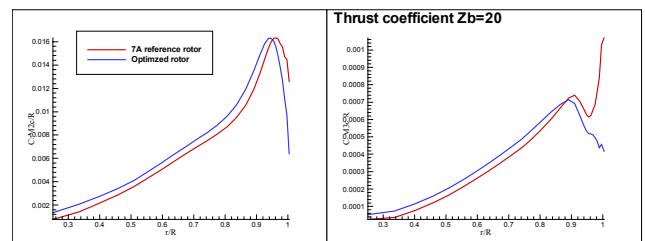


Figure 7: Airloads comparison for the optimization of 7A rotor chord distribution at tip

Sweep distribution optimization

The optimization of the blade tip sweep starting from the 7A rotor has been performed, using both the *elsA* software and the HOST code as flow solver in the optimization process, in order to compare the suitability of both approaches.

Sweep – CFD optimization

As for the chord optimization, the optimization has been performed, using 1 design variable at $r/R=1$ and Bézier curves definition.

In a few optimization iterations, the sweep value at tip is converging to an unusual positive value as shown on Figure 8, up to reach a final value of the tip airfoils displacement of $0.57c^*$ at $r/R=1$, which is corresponding to a swept tip angle of 52° .

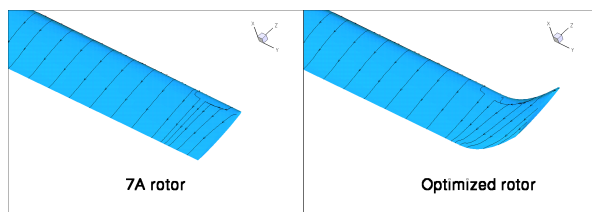


Figure 8: Result of the optimization of 7A rotor swept tip

The improvements of hover performance are illustrated on Figure 9. The maximum Figure of Merit is increased by 0.71 point, which is rather small. Indeed, because of the new sweep distribution, the local relative Mach number is lower than for a straight blade (Figure 10), and by this way the intensity of the shock wave is reduced, leading to better efficiency of the rotor.

One can also notice on Figure 9 that this increase is not constant for all thrust coefficients. The thrust of maximum of Figure of Merit is $Zb=17.8$ for the optimized blade, instead of $Zb=21.5$ for the reference rotor. The new optimized rotor has a very different behavior at high thrust and is much more sensitive to stall. This behavior has not been seen by the optimizer since only the point of maximum of Figure of Merit is optimized (because the collective pitch is always added as a design variable). One can mention also in addition that such a forward swept tip rotor will probably generate dynamic problems. In comparison with a straight blade, the center of pressure in the outer part of the blade is moved forward. And the lift on the swept region of the blade creates a nose-up moment along the length of the blade. This moment will increase the effective collective pitch and twisting, and will increase the sensitivity to stall at high thrust. Even if this effect is not directly taken into account in the optimization chain (rigid blade assumption, no dynamic coupling), the negative effect of such a swept tip is detected, by comparing the thrust coefficient of the design points.

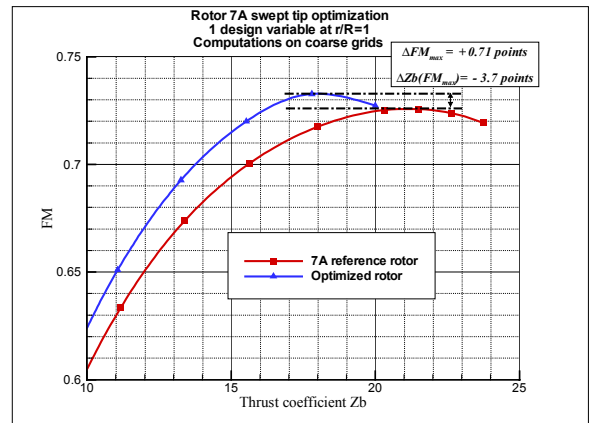


Figure 9: FM/Zb curve of the 7A swept tip optimized rotor

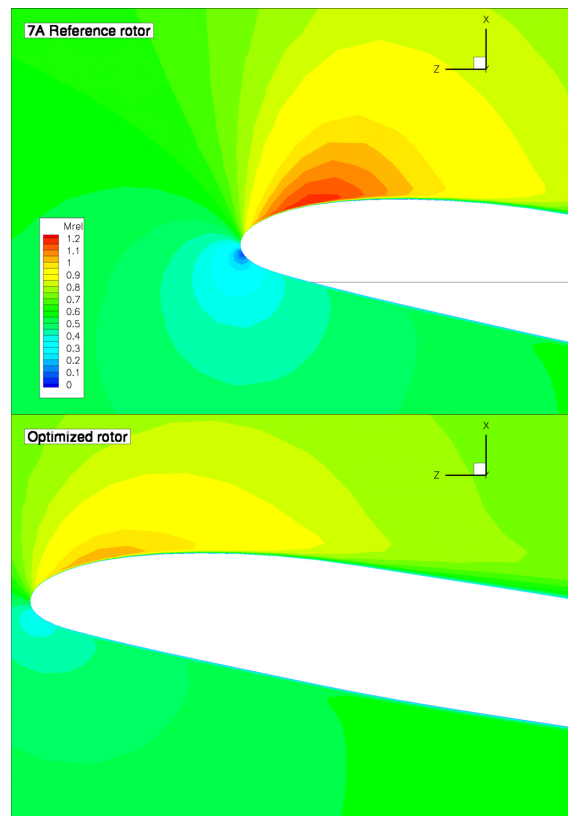


Figure 10: Relative Mach number flowfield around 7A reference rotor and swept tip optimized rotor at $r/R=0.98$ for a thrust coefficient $Zb=18$

Sweep – Lifting-line optimization

The same optimization of 7A rotor swept tip has been performed using HOST as the flow solver. And as shown on Figure 11, some difficulties have been encountered.

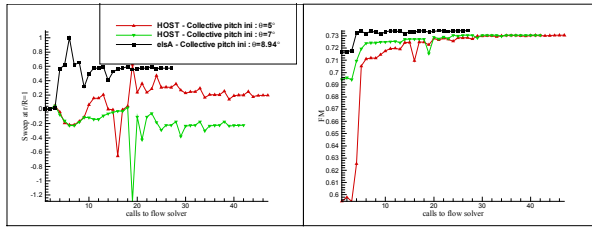


Figure 11: Comparison of 7A rotor swept tip optimization

The convergence history of the design variable representing the sweep at $r/R=1$ shows that both optimizations with *elsA* and HOST do not reach the same result. In addition the optimization performed with the HOST code shows that depending on the starting point on the FM/Zb curve (by modifying the initial collective pitch), the optimization result is either a forward swept tip or totally on the opposite a backward swept tip.

The high dependence of the starting point, and the difficulties to compute small variations effect for the gradient calculations (erratic design variable convergence) of the lifting-line solver in comparison with the CFD solver justifies not to use the HOST code method in such optimization procedure.

For all further optimizations presented here, only the results obtained by using *elsA* are considered of interest.

Anhedral distribution optimization

One important characteristic of a rotor for its efficiency in hover, is its anhedral and especially at tip. Two optimization runs have been performed on the anhedral distribution starting from the 7A rotor blade tip. The first run has been conducted without any constraint or limitation on the value of the anhedral at tip. The second run has been done in limiting the anhedral tip angle through an optimization constraint, in order to avoid unrealistic value for the anhedral at blade tip.

The two optimizations performed on the 7A rotor anhedral tip are presented in the following table:

case	Design variables	location (r/R)	Anhedral tip angle constraint
OPT1	1	1	no
OPT2	2	0.95 and 1.0	Yes

In both optimizations the rotor geometry is unchanged for $r/R < 0.90$. No bounds are imposed on the design variable for OPT1, and for OPT2, the value of the maximal anhedral tip angle is set to -30° .

The results of these optimizations are presented on Figure 12.

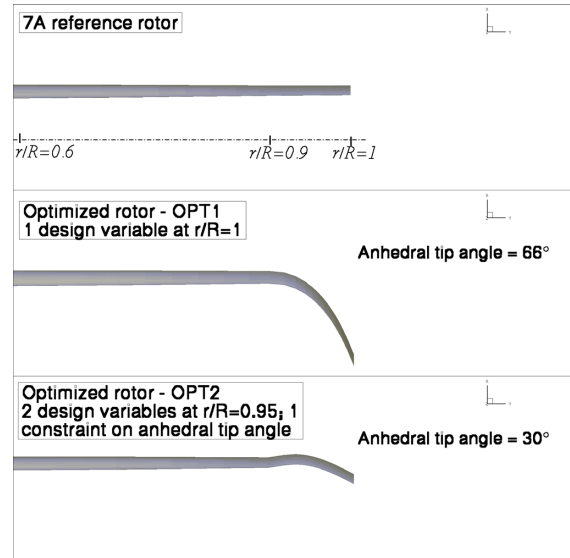


Figure 12: Optimizations of 7A rotor anhedral at tip

As expected both optimizations are leading to a strong downward (negative) anhedral at tip. Without any limitations on the value of the blade tip anhedral, the optimized blade (OPT1) presents a very strong anhedral (-66° at tip). This new anhedral distribution is linked with an important improvement of the rotor efficiency in hover, as shown on Figure 13. The maximum Figure of Merit is improved by 1.67 points and this maximum is strongly shifted to higher loads ($\Delta Zb = +3.5$).

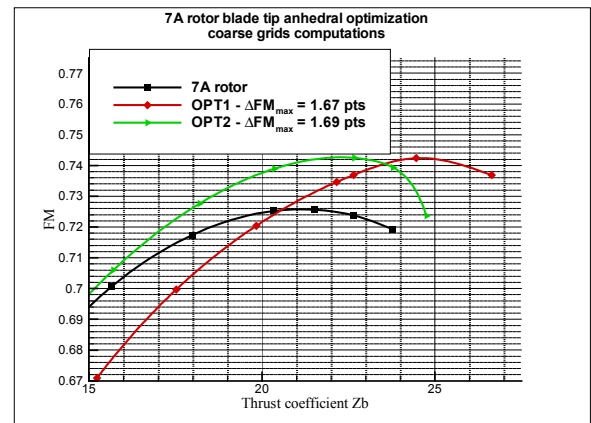


Figure 13: FM/Zb curves of the 7A blade tip anhedral optimizations

This benefit of the tip anhedral for hover efficiency is mainly explained by the position of the tip vortex emission located below the main part of the blade. Due to the wake contraction, the blade vortex interaction is reduced. This is illustrated by the vorticity field around 7A reference rotor and OPT1 optimized rotor (Figure 14). The relative velocity streamlines are representing the vortex trajectory; it can be clearly seen that the vortex emitted by the OPT1 rotor tip is convected

downstream far from the lower surface of the following blade. The blade-vortex interaction is strongly reduced. The intensity of the vortex emitted by the reference rotor and the OPT1 rotor are also quite different. Additionally, because of the anhedral, the lift is reduced in the outer part of the OPT1 blade.

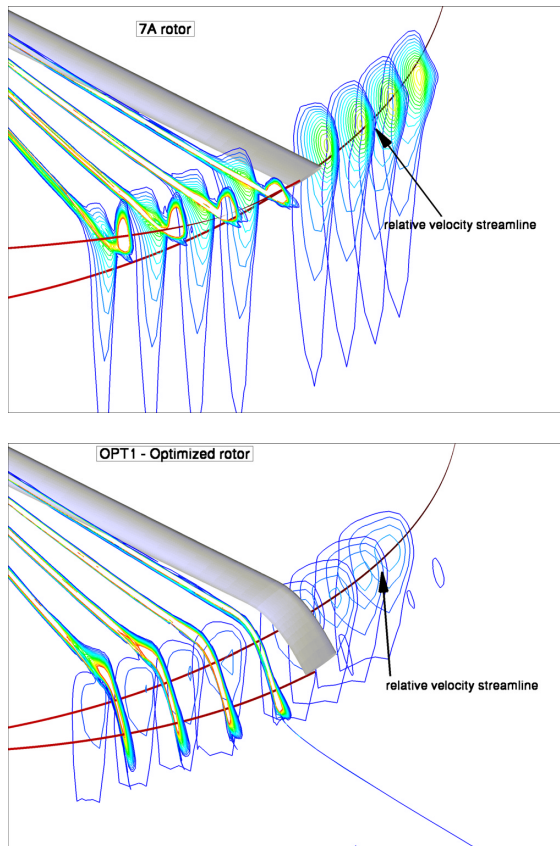


Figure 14: Vorticity contours and relative velocity streamlines comparison for 7A reference rotor and anhedral tip optimized rotor

Nevertheless, the OPT1 performance at low thrust are weaker than those of the 7A reference rotor. Indeed, the comparison of the FM/Zb curves of the reference and of OPT1 rotor (Figure 13) suggests that there could be a solidity effect explaining the shift of the FM/Zb curve towards high thrust coefficients. And in fact, even if the chord law of the rotor is unchanged, the real surface of the blade is increased because of the very strong anhedral at tip. This increase of the rotor solidity is approximately of 5% whereas the Zb of FM maximum is increased by more than 10%, so the solidity effect cannot explain all the differences in Zb of FM_{max}. It remains that the OPT1 geometry is certainly unrealistic on a structural basis.

One way to limit a too strong anhedral is to impose geometric bounds or optimization constraints, that have been used on the second optimization (OPT2) for which the anhedral tip

angle is limited to -30° . For this optimization, 2 design variables are used at $r/R=0.95$ and $r/R=1$. The resulting OPT2 rotor is presented on Figure 12. The final blade anhedral tip angle is much reduced and the final value of the anhedral tip angle is -30° , the maximum allowed by the optimization constraint. Consequently the increase of the rotor solidity is very small and can be neglected. The blade presents an unusual positive then negative anhedral that allows to have a longer anhedral distance for a limited value of the anhedral tip angle.

The FM/Zb curve, plotted on Figure 13 shows an improvement of 1.69 points of the maximum Figure of Merit. In contrary to the OPT1 rotor, this maximum is only slightly shifted to high thrust while the performance at low thrust of the OPT2 rotor is better than the reference rotor performance. This is achieved thanks to the positive/negative anhedral.

These optimizations show the importance of the choice of the geometric restriction to impose during the optimization loops. Even if a strong anhedral is good for hover efficiency, it is better to limit the blade to reasonable deformation. It can be done with the geometric bounds by reducing the research space for the optimizer, or through optimization constraints (like the limitation of anhedral tip angle) that enable to control the optimization result.

These first optimizations initialized by the 7A/7AD rotor geometries are demonstrating the good capability of the optimization chain to reach new blade geometries with improved aerodynamic performance in hover. Nevertheless caution has to be taken to avoid unrealistic results.

Applications on ERATO rotor

ERATO (Figure 15) is a rotor initially designed in the framework of a cooperative program between ONERA, DLR and Eurocopter which aims to understand and reduce the noise generation of rotor blades (Ref 16, 17). It has been demonstrated after wind tunnel tests that the ERATO rotor generated lower noise levels than the 7A/7AD rotors. However, the hover performance of the ERATO rotor where not as good as the 7AD rotor. In particular, an aerodynamic deficiency was observed at high thrust coefficients. The characteristics of the ERATO rotor are similar to those of the 7A/7AD rotors, and thus its radius is of 2.1m for a Mach tip number equal to 0.617. The linear aerodynamic twist is $\tau = -10^\circ/R$.

The next paragraphs present the optimization of hover aerodynamic efficiency, of new rotors starting from the ERATO rotor geometry.

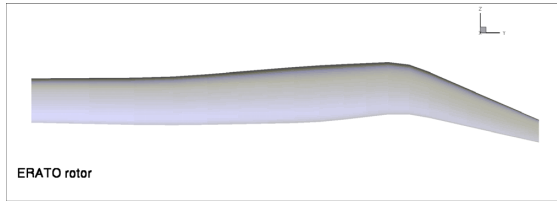


Figure 15: ERATO rotor planform

Blade tip optimization

An optimization of the ERATO blade tip is performed here. The rotor geometry is unchanged for $r/R < 0.9$ and 3 design variables are used at $r/R=1$: chord, anhedral and geometric twist. The bounds of each design variable have been chosen in order to avoid reaching unrealistic values. The lower bound of the chord has so been set to $0.3 c^*$; the anhedral is limited using the optimization constraint on anhedral tip angle, which is set to -15° . And the lower bound of the geometric twist is set at -9° (-7.83° for the reference rotor).

The resulting planform is presented on Figure 16. The optimized blade has a negative anhedral at tip and the final value of the anhedral tip angle is 15° , (the maximal value authorized). The chord has slightly been reduced at $r/R=1$, but because of the use of Bézier curve, the blade tip chord law is quite different from the reference rotor. In addition the twist at tip has been increased up to -9° , equal to the lowest bound.

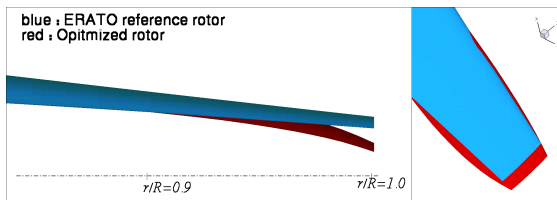


Figure 16: ERATO blade tip optimized rotor

The aerodynamic performance computed on fine grids ($k-\omega$ SST model) for the optimized rotor shows an important improvement of 4.15 points of maximum of Figure of Merit (Figure 17). Moreover, the thrust at FM_{max} is higher ($\Delta Zb=+2.85$).

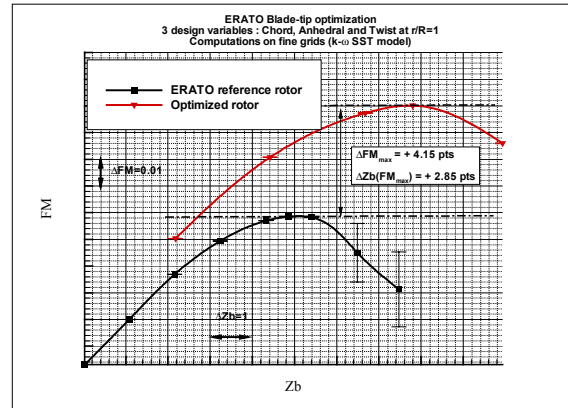


Figure 17: FM/Zb curve of ERATO blade tip optimized rotor

Most of the gain of efficiency in hover is due to the anhedral at tip as explained previously for the optimization of 7A tip anhedral. The increased twist at tip has also an important influence on hover performance. This examples proves that the developed optimization chain is able to treat simultaneously several different blade shape parameters. The final optimized rotor shows very good aerodynamic performance, compared to the reference.

Multi design variables optimization

All the optimizations presented up to now in the present paper have been performed with only a few design variables. The last application of the optimization chain is a more complex optimization coupling several blade shape parameters. 8 design variables are used to modify the ERATO blade geometry : chord and anhedral at $r/R=1$, sweep at $r/R=0.8$ and $r/R=1$ (from $r/R=0.45$ as the ERATO reference rotor) and 4 design variables on the twist distribution in the main part of the blade. No optimization constraint is activated, but the rotor solidity has to remain constant with the modification of the chord distribution.

After a few optimization iterations, the process converges to a planform very far from the reference (Figure 18). The forward/backward sweep has almost disappeared, and the new planform is quite straight, except at the blade tip, where a slight swept tip has been retained. At the blade tip, the blade has a strong negative anhedral (-35° for the anhedral tip angle), and the chord has been slightly reduced. The final twist distribution is also quite similar and the value of the twist at tip has been kept constant.

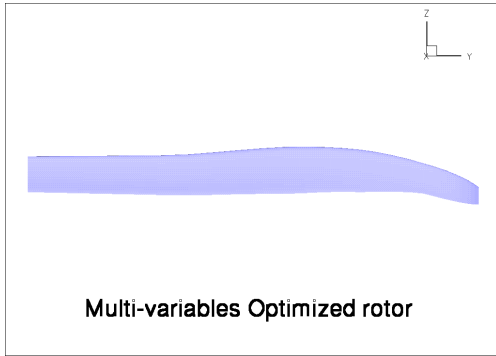


Figure 18: ERATO multi-design variables optimized rotor

The FM/Zb curve of this new optimized rotor (Figure 19) shows a spectacular improvement of the rotor efficiency in hover. The maximum of Figure of Merit is increased by 4.95 points and this maximum occurs at a much higher thrust coefficient ($\Delta Zb=+4.65$). The problem of premature stall observed on the ERATO rotor is completely solved. This is illustrated on Figure 20, on which one can see that for $Zb=16$ (maximum of FM for ERATO rotor) a large separation appears at tip for the reference blade. On the contrary, for the same thrust coefficient, there is no separation at the tip of the optimized rotor. Moreover at $Zb=20.5$ (maximum of FM for the optimized rotor), no large separation is yet present, which indicates that the stall will occur at even higher thrust coefficients. As the airfoils used to define both rotors at tip are the same, the differences are only due to the modification of the planform given by the optimizer. The strong anhedral is surely responsible for most of the gain of aerodynamic efficiency regarding the result of the previous optimizations.

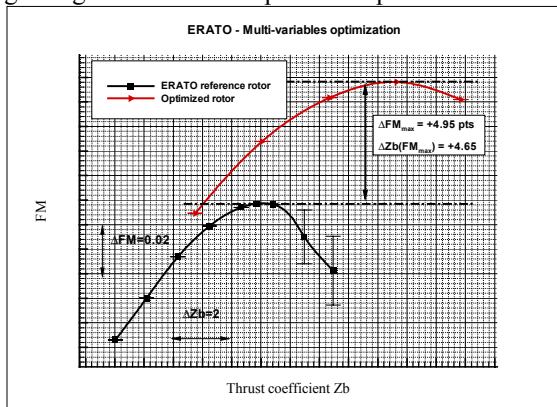


Figure 19: FM/Zb curve of the ERATO multi-design variables optimized rotor computed on fine grids

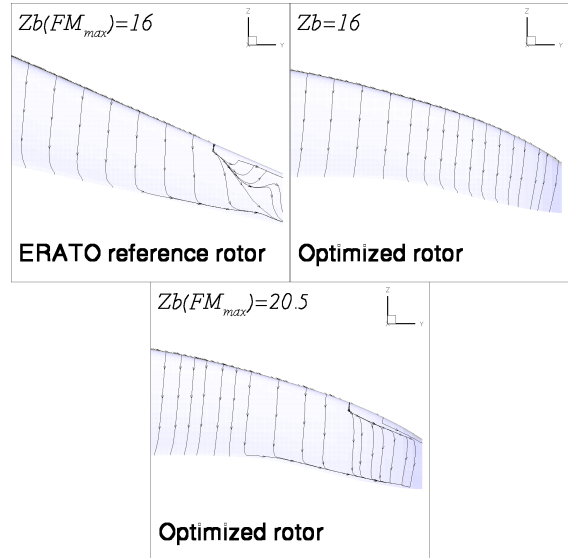


Figure 20: Friction lines comparison between ERATO and optimized rotor for different thrust coefficient

Conclusion

A numerical optimization procedure for improving the aerodynamic performance of hovering helicopter rotors has been presented. The optimization process is based on the coupling of a gradient algorithm (CONMIN) with a 3D Navier-Stokes solver (*elsA* software) and a lifting-line code (HOST). Both rigid and soft blade assumptions can be used.

The application of this optimization chain to the modification of 7A/7AD rotor linear aerodynamic twist, chord distribution, sweep distribution, or anhedral distribution shows a good capability of the method to reach new rotor planforms and geometries with improved aerodynamic performance.

These first applications have shown that the lifting-line method is not reliable enough to be used in such an optimization chain. In addition, it has been found with the Navier-Stokes computations that the range of the modifications realized by the optimizer has to be limited by geometric bounds or optimization constraints.

The optimization chain applied to the modern geometry rotor ERATO leads to a consequent improvement of hover efficiency. In particular the premature stall of ERATO in hover may be improved significantly either by optimization of the blade tip or by a global multi design variables optimization.

These applications demonstrate the good efficiency of the method and its suitability to be used to design new rotor geometries. Even if hover is a critical flight condition for helicopter, other flight conditions should be taken into account to design a new rotor. In consequence, future work will be focused on multi-point optimization strategy

that would optimize simultaneously hover and forward flight performance.

Acknowledgment

The authors would like to acknowledge the French Ministry of Transport (DPAC) and SPAé for the financial support of the numerical studies presented in this paper.

References

- [1] Walsh, J. L., Bingham, G. J., Riley, M. F.: *Optimization Methods Applied to the Aerodynamic Design of Helicopter Rotor Blades*, Journal of the American Helicopter Society, Vol 32(4), Oct. 1987, pp39-44
- [2] Lim, J., Chopra, I.: *Aeroelastic optimization of a helicopter rotor*, 44th American Helicopter Society Forum, Washington DC, June 1988
- [3] Rocchetto, A., Poloni, C.: *A Hybrid Numerical Optimization Technique Based on Genetic and Feasible Direction Algorithms for Multipoint Helicopter Rotor Blade Design*, 21st European Rotorcraft Forum, Sept. 1995
- [4] Zibi, J.: *An Optimization Method Applied to the Aerodynamics of Helicopter Rotor Blades*, 21st European Rotorcraft Forum, Sept. 1995
- [5] Mialon B., Fol, T., Bonnaud C.: *Aerodynamic optimization of subsonic flying wing configurations*, 20th AIAA Applied Aerodynamics Conference, Saint Louis (USA), June 2002
- [6] Tursi, S.: *Transonic wing optimization combining genetic algorithm and neural network*, 21st Applied Aerodynamics Conference, Orlando, June 2003
- [7] Gauger, N. R.: *Aerodynamic shape optimization using the adjoint Euler equations*, 2001 Logos Verlag, Berlin, ISBN 3-89722-683-9, pp 87-96
- [8] Soemarwoto, B. I., Laban, M., Jameson, A., Martins, A. L., Oskam, B.: *Adaptative aerodynamic optimization of regional jet aircraft*, 40th AIAA Aerospace sciences Meeting and Exhibit, Reno, January 2002
- [9] Chung J., Lee K. D.: *Shape optimization of transonic compressor blades using quasi-3D flow physics*, ASME TURBEXPO, 2000-GT-0489, Munich, May 2000
- [10] Burguburu, S., Le Pape, A.: *Improved aerodynamic design of turbomachinery bladings by numerical optimization*, ONERA-DLR Aerospace Symposium, June 2002
- [11] Vanderplaats, G. N.: *CONMIN – a fortran program for constrained function minimisation*, NASA TMX 62283, 1973
- [12] Cambier, L., Gazaix, M.: *elsA : an efficient object-oriented solution to CFD complexity*, paper no 2002, 40th AIAA Aerospace Sciences Meeting and Exhibit, Reno 2002
- [13] Benoit, B., Dequin, A.-M., Kampa, K., Grunhagen, W., Basset, P.-M., Gimonet, B.: *HOST, A General Helicopter Simulation Tool for Germany and France*, American Helicopter Society, 56th Annual Forum, Virginia Beach, May 2000
- [14] Bézier, P.: *Essais de définition numérique des courbes et surfaces expérimentales*, Thèse de doctorat d'état, février 1977
- [15] Beaumier P., Chelli E., Pahlke K.: *Navier-Stokes prediction of helicopter rotor performance in hover including aero-elastic effect*, 56th American Helicopter Society Forum, Virginia Beach (USA), May 2000
- [16] Splettstoesser, W., Van der Wall, B., Junker, B., Schultz, K., Beaumier, P., Delrieux, Y., Leconte, P., Crozier, P.: *Wind Tunnel Test Results and Proof of Design for an Aeroacoustically Optimized Rotor*, 25th European Rotorcraft Forum, Sept. 1999
- [17] Prieur, P., Splettstoesser, W.: *ERATO – an ONERA-DLR Cooperative Programme on Aeroacoustic Rotor Optimisation*, 25th European Rotorcraft Forum, Sept. 1999